

Seasonal and interannual changes of significant wave height in shelf seas around India during 1998 to 2012 based on wave hindcast

**V. Sanil Kumar^{1*}, Jossia Joseph², M.M. Amrutha¹, B.K. Jena², K.M. Sivakholundu²,
K.K.Dubhashi¹**

¹Ocean Engineering Division, CSIR-National Institute of Oceanography (Council of Scientific & Industrial Research), Dona Paula, Goa 403 004 India

²Coastal and Environmental Engineering Division, National Institute of Ocean Technology, Pallikaranai, Chennai-600 100, India

*corresponding author: V.S.Kumar email:sanil@nio.org Tel: 0091 832 2450 327 Fax: 0091 832 2450 602

Abstract

Present study examines the interannual changes of significant wave height (H_s) in shelf seas around Indian mainland based on the 15-year (1998 to 2012) wave hindcast data obtained from numerical model. Validation of the hindcast data with buoy-measured data shows that hindcast H_s is reasonably in good agreement with the observation (Pearson correlation coefficient values of 0.92-0.97). Annual average H_s varied from 0.9 to 1.4 m and the wave heights are higher (~20%) in western shelf seas compared to eastern shelf seas. The analysis reveals seasonal fluctuations of wave climate, with a strong influence of Asian summer monsoon in the western shelf seas compared to the eastern shelf seas of India. Maximum H_s varied from 3.65 to 7.36 m and these maximum values were during the tropical cyclones. During 1998 to 2012, a statistically significant positive trend of 0.8 to 1.4 cm yr⁻¹ in annual mean H_s is observed and the increasing trend is higher (~0.7 to 2.5 cm yr⁻¹) during the Asian summer monsoon period (June-September). The average trend of annual mean wind speed is also positive and is higher (~1.67 cm s⁻¹ yr⁻¹) for the western shelf seas than that for eastern shelf seas (~0.93 cm s⁻¹ yr⁻¹).

Key Words: Wind waves, Wave height, Inter-annual variability, Wave hindcasts, Arabian Sea, Bay of Bengal, North Indian Ocean

Introduction

The shelf seas of the Indian subcontinent are being explored for oil and gas and minerals due to the rising demands of these commodities. The wind generated ocean waves play a significant role in all aspects of coastal and offshore activities (Semedo et al., 2013). Waves also cause erosion of the coastlines and the coastline erosion is expected to be intensified by future sea level rise (Hinkel et al., 2013) along with potential changes in the wave climate (Seneviratne et al., 2012). Hence, it is important to know the changes in wave climate in the shelf seas of India. Generally, significant wave height (H_s) is used as an indicator to study the wave climate at a location and the variations in annual mean H_s during different years are examined to know the change in wave climate. Estimating reliable trends in wave height from measured buoy data are limited because they are sparse point measurements and are not available for long period. Hence, the long-term and decadal trend of wave climate in the different parts of major oceans are studied based on voluntary observing ships, global datasets produced within wave reanalysis, satellite altimetry or wave model hindcasts (Carter and Draper, 1988; Allan and Komar, 2000; Gulev and Grigorieva, 2004; Young et al., 2011; Semedo et al., 2011; Appendini et al., 2014; Aarnes et al., 2015).

The waters of the North Indian Ocean (NIO) are exposed to seasonally reversing winds; winds from the southwest (SW) during the Asian summer monsoon period (June to September) and from the northeast (NE) during the winter monsoon period (October to January). These seasonal changes in winds produce similar changes in the surface waves in NIO (Anoop et al., 2015). During the annual cycle, monsoon is the dominant mode of variability and it covers 92 % of the total variability (Anoop et al., 2015). In the NIO, the swell heights are greater than those associated with the wind waves and remote influences propagating from the subantarctic region of the south Indian Ocean are observed (Anoop et al., 2015). The Indian subcontinent divides the NIO into two semi-enclosed seas, the Arabian Sea (AS) and the Bay of Bengal (BoB). AS and BoB, are the only sea areas in the Northern Hemisphere with larger summer than winter energy levels, due to a combination of stronger summer monsoon winds and higher swell influx during southern ocean winter and hence have large seasonality (Barstow et al., 2011). Waves in the BoB are frequently influenced by tropical cyclones, whereas the occurrence of the tropical cyclone in AS is less compared to BoB, and the ratio of their frequencies is around 1:4 (Dube et al., 1985).

In the NIO, the long-term trend in wave height is estimated based on European Centre for Medium-Range Weather Forecasts (ECMWF) global atmospheric re-analysis product (ERA-I) during 1979 to 2012 (Shanas and Kumar, 2014; 2015; Kumar and Anoop, 2015; Anoop et al., 2015; Aarnes et al., 2015) and satellite altimeter data during 1993-2010 (Kumar et al., 2013a), 1992-2012

(Bhaskaran et al., 2014) and 1996-2012 (Hithin et al., 2015). The study using the altimeter data for a period of 18 years in the Indian Ocean indicates that the variation in H_s is almost negligible (Kumar et al., 2013a). Young et al. (2011) based on the 23 year period (1985-2008) satellite altimeter measurements indicate a weak increase (0-0.25% of annual mean value) of H_s in NIO. Anoop et al. (2015) study shows a negative trend of H_s in a small area of the central east coast of India, whereas the study of Young et al. (2011) for the same region shows a small positive trend. Aarnes et al. (2015) study shows that during 1979 to 1991, there is an increase of H_s (0-0.5% of annual mean value per year) in NIO and from 1992 to 2012, there is a decrease (0-0.5%). The study in the central AS based on satellite altimeter data shows a positive trend of 0.63 cm yr^{-1} in the annual mean H_s (Hithin et al., 2015).

The earlier studies (Young et al., 2011; Kumar et al., 2013a; Anoop et al., 2015; Kumar and Anoop, 2015; Aarnes et al., 2015) indicated that the long-term-trend in wave climate is different for different locations in the shelf seas around India. Wave hindcasts with numerical models have become a common tool to get high-resolution (spatial and temporal) long-term wave height for locations devoid of observational data or having short-term measurements (Appendini et al., 2014), as in the north Indian Ocean. Hence, we have examined the trend in the estimated H_s based on the numerical model over the period 1998 to 2012 at the same locations covered in the study of Kumar and Anoop (2015). With the advent of long marine Earth-observing satellite missions (European Remote Sensing Satellites ERS-1 and ERS-2, starting in 1991), the quality and coverage of marine wind speed and H_s observations rose dramatically (Aarnes et al., 2015). Since such observations are usually assimilated into global reanalyses, the quality of a reanalysis before and after the satellite era are different and hence trends in the analysis will be spuriously affected if we combine data before and after 1992 (Aarnes et al., 2015). Hence, we have not carried out the trend for the longer period even though for trends on climate, the rule of thumb is to use data covering 30 years.

In order to understand temporal variations in the wind-driven H_s seasonal cycle, we calculate the trend of monthly average H_s and trends of wind speed as well. The paper is organized as follows. Section 2 provides information on the locations studied, wave model setup and validation by buoy data. Section 3 presents the analysis on significant wave height trends and variability. Discussions are given in section 4 and conclusions of the study are given in section 5.

2. Materials and methods

2.1 Study locations

Nineteen locations considered in the study of Kumar and Anoop (2015) in the shelf seas of India are selected for the present study considering approximately 1.5° spacing in latitude of the locations since Kumar et al. (2012) has shown that the average wave characteristics in the same water depth along the eastern AS do not vary significantly within 200 km distance. The interannual changes in H_s at these locations based on the ERA-I data are reported by Kumar and Anoop (2015). Among these 19 locations, 11 locations are in the western side and 8 locations are in the eastern side of the Indian mainland (Figure 1) and the locations studied are in water depth more than 55 m (Kumar and Anoop, 2015).

2.2 Model setup

The present study is based on the 15-year wave data simulated using the third generation wave model MIKE21 Spectral Waves (SW) (see Sorensen et al., 2004 for model description) for the preparation of the wave atlas of the Indian coast (Sivakholundu et al., 2014). The model is based on the wave action balance equation where the wave field is represented by the wave action density spectrum and the numerical integration of wave action balance equation is formulated in Cartesian co-ordinates (Komen et al., 1994; Young, 1999). The discretization of the governing equation in geographical and spectral space is performed using cell-centered finite volume method. In the geographical domain, an unstructured mesh technique is used. A logarithmic spectral discretization is employed with a minimum frequency of 0.055 Hz, 25 frequencies, and a frequency factor of 1.1. The directional discretization is done for 360° divided in 16 directions. The details of the model equations and methods of solution are explained in the MIKE-21 user manual (DHI, 2011). The bathymetry of the study area was prepared using the ETOPO1 (Earth Topography-1 minute) (Amante and Eakins, 2009) and MIKE-CMAP data. MIKE CMAP works with data from digital nautical charts. Using this one can create a bathymetry of the coastal region in the world. The model wind forcing is provided by ECMWF operational archive wind data (Trenberth, 1992) at every six hours interval (<http://browse.ceda.ac.uk/browse/badc/ecmwf-op>). These data sets are produced at ECMWF as part of various global analyses and forecasts and archived in MARS (Meteorological Archival and Retrieval System). ECMWF analysed wind from operational archive is available with a variable grid at every six hour interval. Bilinear interpolation is carried out on the input wind data to match the model time step. The time step of the simulation is 300 s. The resolution and internal representation of the archive vary according to changes in data assimilation and forecast system in operational use at ECMWF. The spatial resolution of the wind data used in the present study is 0.5° from 1 January 1998 to 31 January 2006, 0.25° from 1 February 2006 to 30 January 2012 and 0.125° from 1 July 2012 to 31 December 2012. Even though the wind data is with non-homogenous spatial

resolution, the product is successfully utilised by ECMWF for various operational activities. The wind data set is validated with measured data, which exhibits good correlation.

Considering the complex variation in bathymetry and the demand for a high resolution in the model, extensive sensitivity analysis is carried out. It is observed that inclusion of Gulf of Thailand and Java Sea significantly increases complexity and run time of the model without much improvement in the model results in NIO. Hence, the model domain is closed in the Malacca strait. However, the Red Sea and the Arabian Gulf are included in the domain. The selection of southern boundary seems to be very sensitive and is fixed at 40° S (Longitude varying from 20 to 120° E) after extensive analysis. The sensitivity analysis is carried out with varying southern boundary from 30° S to 70° S at an increment of 10° (i.e., 30° S, 40° S, 50° S, 60° S and 70° S). The simulation is carried out 10 months from January to October 2005 with the same wind input and same model setup except the model domain. The model results are validated with two deep sea observations in NIO (one in the AS and another in the BoB). The model results are statistically compared with measured buoy data using Pearson's linear correlation coefficient (r), root-mean-square error (RMSE), and mean absolute error (MAE) and the results are presented in Table 1. Considering the error estimates and the complexity of the southern ocean topography and time constraints, the southern boundary of the model setup is fixed at 40° S.

$$r = \frac{\sum_{i=1}^N |(A_i - \bar{A})(B_i - \bar{B})|}{\sqrt{\sum_{i=1}^N |(A_i - \bar{A})^2 (B_i - \bar{B})^2|}} \quad (1)$$

$$MAE = \frac{1}{N} \sum_{i=1}^N |(A_i - B_i)| \quad (2)$$

$$RMSE = \sqrt{\frac{1}{N} \sum_{i=1}^N (A_i - B_i)^2} \quad (3)$$

Where A_i represents the parameter based on the numerical model, B_i represents the measured parameter, N is the number of data points, and the overbar represents the mean value.

2.3 Model validation

The measured wave data collected using a moored Seatex buoy (Oceanor, Norway) under the National Data Buoy Programme (Premkumar et al., 2000) at 1 location in the AS (AD02 15.00° N; 69.01° E) during February-December 2012 and 1 location in the BoB (DS3 12.15° N; 90.75° E)

during January-December 2003 are used for comparison with the hindcast H_s value. The heave data of the buoy is recorded at 2 Hz interval for 17 minutes duration and from the recorded heave data, the wave spectrum is obtained through fast Fourier Transform and the H_s is estimated from the zeroth spectral moment (m_0) as $H_s = 4\sqrt{m_0}$.

Comparison of hindcast H_s data with the measured data in AS at location AD02 for the year 2012 indicates that hindcast data is reasonably in good agreement with the observation (Figure 2a). The scatter plots are reasonably tight, with high Pearson correlation coefficient (r) of 0.97 for the H_s with bias value of 0.13 m, scatter index (SI) is also small (0.16). The monthly mean hindcast H_s is within 15% error of the measured value. During the year 2012, the difference between the average value of the H_s between the measured and hindcast data is 0.13 m, whereas the difference between the maximum H_s value is high (~ 0.55 m) and the difference in the 90 percentile H_s is 0.34 m. Figure 2b shows that the model underestimates the H_s data in BoB for the year 2003 (Figure 2b). The Pearson correlation coefficient for the H_s is 0.92 with bias value of 0.3 m and low scatter index (SI) values (0.23). Scatter index is calculated by dividing the RMSE with mean of the measured value and it gives the expected error for the H_s . During the year 2003, the difference between the average value of the H_s between the measured and hindcast data in BoB is 0.36 m, whereas the difference between the maximum H_s value is 0.29 m and the difference in the 90 percentile H_s is 0.4 m. In BoB, the monthly mean hindcast H_s in some months deviates more than 15% of the measured value. The scatter plot of the H_s based on wave hind cast results obtained without closing the southern boundary and that obtained by closing the southern boundary at 40° S during February - December 2012 at a location in the AS (AD02 15.00° N; 69.01° E) is presented in Figure 3. Closing the southern boundary at 40° S results in underestimation of the wave height (RMSE=0.21 m) and is mainly for lower wave heights ($H_s < 2$ m). The influence of swells from the southern ocean on the waves in the north Indian Ocean can vary with location and season. The comparison of the hindcast H_s , mean wave period and mean wave direction for Vijayadurg in the coastal Arabian Sea and Cuddalore in the coastal Bay of Bengal is carried out with the one-year measured waverider buoy data and presented in Sivakholundu et al. (2014).

2.4 Trend estimate

The trend of H_s is estimated based on the slope of the linear best-fit curve to the annual mean/monthly mean H_s for 15 years. A positive slope indicates H_s increase and negative slope an H_s decrease. The linear trends in H_s for 1998 to 2012 are also calculated for summer monsoon, winter monsoon and non-monsoon seasons separately. The significant trend of the H_s is estimated by

applying Kendall's Tau-Sen test (Sen, 1968; Burkey, 2006; <http://www.mathworks.com/matlabcentral/fileexchange>).

3. Results

3.1 Variations in H_s

The monthly mean H_s indicates that the influence of summer monsoon is high at all locations in the western shelf seas of India and is not significant at locations 12 to 15 in the eastern shelf seas of India (Figure 4). Hence, the monthly mean H_s is high in July at all locations studied except at locations 12 to 15 (Table 2). The average H_s during July along the western shelf seas of India varied from 2.1 to 2.7 m. For locations 12 to 15 in the eastern shelf seas of India, the H_s is high in December due to NE winds of the winter monsoon. The locations 12 to 15 are in the shadow regions of the southern part of Indian and the Sri Lankan land mass and hence, relatively low waves are observed at these locations during the summer monsoon. Anoop et al. (2015) have observed that the Sri Lankan landmass has a major role in the wave climate of a major part of the eastern shelf seas of India.

The average H_s during three different seasons is presented in Figure 5. In the non-monsoon period, the waves in the shelf seas of India become low in height (H_s range from 0.6 to 1.2 m) due to a lower wind speed over the basin (Anoop et al., 2015) (Figure 5a). The average H_s in the shelf seas of India during summer monsoon is high (H_s varies from 0.6 to 2.5 m and the average H_s is higher (~ 1.8-2.5 m) off the central west coast of India (Figure 5b). During the summer monsoon, due to the strong cross-equatorial winds of the Findlater (Somali) Jet (Findlater, 1969), wave heights are high in the central AS. Due to the sheltering effect of the Sri Lankan land mass, the average H_s is less than 1 m in the coastal region of the southeast coast of India. The wave height in the shelf seas of India during the winter monsoon period is slightly higher than it is in the non-monsoon. During the winter monsoon period, high waves (1-1.2 m) are observed off the southern coast of India (Figure 5c). The wave height in the BoB is higher (~ 0.8-1.2 m) than that in the AS (~0.6-1.0 m) during the winter monsoon period due to the northeast monsoon winds.

The mean H_s during the summer monsoon is highest (~ 2.1 m) at locations 2 and 3 and is lowest (~ 1 m) at locations 14 and 15 (Table 3). In the study area, during the summer monsoon period, maximum H_s (~7.36 m) is observed at location 2 in the western shelf seas of India (Figure 6). During the winter monsoon and non-monsoon period, seasonal average H_s at all locations is in the range of 0.6 to 1.2 m.

The annual mean H_s during 1998 to 2012 in the shelf seas of India varied from 0.9 m to 1.4 m. Annual mean H_s is highest (~ 1.4 m) at the southern location 11 since the wave height at this location is relatively high during non-monsoon and winter monsoon seasons (Table 3). In the western shelf seas of India, the maximum H_s at different locations during the study period varied from 3.65 m (at location 11) to 7.36 m (at location 2). At most of the locations in the AS, the maximum H_s was in June 2007 due to the super cyclonic storm Gonu, which was the strongest TC on record in the AS. At location 5, high H_s was also observed in June 2004 due to a deep depression (ARB02). In the eastern shelf seas of India, at the southern locations (12 and 13), the maximum H_s were during the TC Thane (December 2011). During the TC Thane, maximum H_s of 6 m is measured off Puducherry, eastern shelf seas of India (Kumar et al., 2013b) and the maximum H_s estimated at location 13, which is in the TC Thane track is 5.86 m. At this location, the model estimated value is close ($< 3\%$ error) to the measured value. At locations 14 to 16, the maximum H_s was during TC Laila (May 2010) and at the northern locations (17 to 19), maximum H_s was during June 2007.

3.2 Long-term variation in seasonal and annual average H_s

Long-period changes in monthly wave activity can be characterized by trends in monthly mean H_s . Trends in monthly H_s show intra-annual variability, but no distinct cycle; in western shelf seas of India (locations 1 to 7), trends are largest and positive in June to September and negative in May (Table 4). In the north of eastern shelf seas (locations 16 to 19) also the trends are largest and positive during June to September. The positive trend is relatively high at all locations in September, except at locations 12 to 15. At locations 12 to 16, the positive trend is high in May.

Long-term changes in wave activity can be characterized by trends in annual mean. The results from the linear trend analysis of annual averages in Figure 7 reveal significant linear trends at all locations. All locations show positive trend (0.82 to 1.47 cm yr^{-1}) in annual average H_s (Table 5). The estimated trends at half of the locations are statistically significant with 90% confidence limit except at 3, 5 to 11 and 19. At location 1, the increasing trend based on ERA-I data is 0.11 cm yr^{-1} , whereas the trend based on the present data is 1.2 cm yr^{-1} . Shanas and Kumar (2014) observed a negligible positive trend (~ 0.012 cm yr^{-1}) in annual mean H_s based on ERA-I data for shallow water location in western shelf seas. The difference in the trend estimated based on the present data and the ERA-I data (Kumar and Anoop, 2015) for the same locations is due to the fact that wave data in ERA-I are produced on a grid with resolution of the order of 110 km and this resolution is inadequate to resolve tropical cyclones and hence high waves are underestimated (Kumar and Naseef, 2015). Figure 8 shows the comparison of H_s estimated based on numerical model and the ERA-I for the locations studied. At all locations except at 8 to 11, the ERA-I H_s are underestimated during the high

waves due to the fact that ERA-I underestimates the upper percentiles (Stopa and Cheung, 2014). The maximum H_s at locations 8 to 11 are less than that at other locations along the western shelf seas of India and hence large underestimation is not observed in the ERA-I H_s (Figure 6). Since the satellite data is already assimilated in the ERA-I, a separate comparison of hind cast data with satellite data is not attempted.

Trend analysis of seasonally average H_s indicates that the monsoon trends are significantly higher than the trends of annual average while non-monsoon trends tend to be significantly smaller (Table 5). The average trend of mean H_s during monsoon in western shelf seas is higher ($\sim 1.8 \text{ cm yr}^{-1}$) than that ($\sim 1.5 \text{ cm yr}^{-1}$) for the eastern shelf seas of India. Performing mean and trend analyses for wind speed for the 1998 to 2012 period reveals seasonal cycles with highest wind velocities in summer monsoon and also large trends in wind speed in summer monsoon. Annual mean wind speed shows the positive trend at some locations, negative trend at some other locations. The average trend of annual mean wind speed for all the locations in the western shelf seas is $1.67 \text{ cm s}^{-1} \text{ yr}^{-1}$ and that for the eastern shelf seas is $0.93 \text{ cm s}^{-1} \text{ yr}^{-1}$ (Table 5).

4. Discussions

The mean H_s during summer monsoon at all the locations in the western shelf seas is 2.0 m, whereas that for the eastern shelf seas is 1.3 m. Kumar and Anoop (2015) reported maximum H_s of $\sim 6.3 \text{ m}$ at locations 5 and 6, whereas the present study shows a value of 6.2 m. Similar to the observation of Kumar and Anoop (2015) the influence of summer monsoon swells at locations 1 to 7 is higher than that at other locations. The mean H_s at all locations in the eastern shelf seas ($\sim 0.9 \text{ m}$) are slightly higher than that in the western shelf seas ($\sim 0.8 \text{ m}$) during the winter monsoon, indicating the predominance of winter monsoon in the eastern shelf seas. The annual mean H_s for all the locations in the western shelf seas ($\sim 1.2 \text{ m}$) is slightly higher than that for the locations in the eastern shelf seas ($\sim 1.0 \text{ m}$) due to the stronger influence of summer monsoon in the AS compared to BoB. The measured data also indicate that the maximum H_s in the eastern shelf seas are less than that in the western shelf seas except during the tropical cyclone (TC) period (Kumar et al., 2010).

During 1998 to 2012, the average trend of annual mean H_s for all the locations in the western shelf seas is 1.14 cm yr^{-1} (0.95% of the annual mean per year) and that for all the locations in the eastern shelf seas is 1.03 cm yr^{-1} (1.03% of the annual mean per year). Based on the 23 year period (1985-2008) satellite altimeter measurements, Young et al. (2011) finds a weak increase (0-0.25% of annual mean value) of H_s in NIO. Trends obtained in the present study are higher than that of Young et al. (2011), which probably is an effect of the different time periods used and the different data sets.

The increase in annual mean wind speed (0.32% of the annual mean in western shelf seas and 0.17% for the eastern shelf seas) is less than that of annual mean H_s . The study of Semedo et al. (2013) shows that wave heights are highest in the Indian sector of the Southern Ocean, southwest of Australia, where the climatological annual mean maxima reach values higher than 5 m. The increasing trend in H_s in As and BoB is due to the increase in H_s observed by Hemer et al. (2010) in the Indian Ocean sector of Southern Ocean. The earlier studies indicated propagation of swells from the Southern Ocean to NIO (Glejin et al., 2013; Nayak et al., 2013). Since the waves in the NIO are mainly the swells arriving from the South Indian Ocean, the increase in H_s observed in the present study is largely due to the increase in swells in the South India Ocean. Bhaskaran et al. (2014) reported that the maximum H_s over the Southern Ocean increased during 1992-2012 and these swells influenced the waves in certain sectors of the NIO. The present study shows that the most significant rate of annual mean H_s increase (1.4 cm yr^{-1}) occurs at the locations 2, 11 and 17. The error in the H_s obtained from hindcast data are upto 15%. Since the trends observed are small ($\sim 1\%$ of the annual average value), slight changes in the annual mean H_s value can alter the trends.

The maximum value of H_s measured by buoy BD11 (14.2° N , 82.93° E) during TC Thane in December 2011 is 5.21 m, whereas that estimated based on the wave model used in the present study is 4.06 m (Figure 9). Even though the correlation coefficient is 0.95, the study shows that the TC generated H_s are underestimated ($\sim 23\%$) by the numerical model since the short-term sub-synoptic scale wind pulses and fluctuations are not likely to be captured by the numerical model to the accuracy required. Similarly, the mean wave period (T_{m02}) is also underestimated by the model (Figure 9). The mean value of measured T_{m02} is 5.6 s, whereas the model estimated value is 5.0 s. Amrutha et al. (2014) reported maximum H_s of 7.3 m in the eastern shelf seas of India off Gopalpur during the TC Phailin. The average H_s during February-October off Gopalpur including the TC Phailin is 1.3 m and the average H_s excluding the TC is 1.26 m (Kumar and Naseef, 2015). During the TC Thane, maximum H_s of 6 m is reported off Puducherry, eastern shelf seas of India (Kumar et al., 2013b). The annual H_s off Puducherry in 2011 is 0.77 m including the TC Thane and is 0.75 m excluding the TC (Kumar and Naseef, 2015). Even though the change in annual average H_s due to tropical cyclone is 2 to 4 cm, it can influence the long-term trend in annual average H_s since the H_s during TC are not estimated accurately.

Even though the wave model hindcasts has comprehensive spatial coverage, the model results heavily depend on the winds used for forcing the model. A 10% error in the estimate of surface wind speed can lead to a 10-20% error in H_s (Cavaleri, 1994). Any bias in the wind data used in hindcasting the waves will result wrong estimation of trends of H_s . For the study area, it was

observed that there is a bias in the ECMWF wind used to force the wave hindcast model. During 1998, the average wind speed measured at buoy location DS01 (15.5°N, 69.2°E) is 5.66 m/s, whereas the average wind speed obtained from ECMWF for the collocated points is 5.58 m/s indicating underestimation in the ECMWF wind speed data by 1.4%. During 2011 and 2012, the ECMWF wind data overestimated the buoy measured wind speed at location AD02 (close to DS1) by 15.7 and 12% respectively (Table 6). The comparison shows that the bias in the ECMWF wind speed data is negative ($\sim 0.08 \text{ m s}^{-1}$) during 1998 and is positive ($\sim 0.85/0.68 \text{ m s}^{-1}$) in the recent years (2011/2012). The varying bias in the ECMWF wind speed data may be also due to the non-homogenous spatial resolution. The varying bias in the ECMWF wind speed data used for forcing the wave model also will contribute to the observed positive trend of H_s apart from the increase caused due to the swells from the Southern Ocean.

The study shows that the H_s obtained by selecting the southern boundary at 40° S is slightly less than (RMSE=0.21 m) that obtained without any restriction on the southern boundary. One might also miss some major high wave events (like kallakkadal events/rogue waves) if the boundary is at 40° S (Patra and Bhaskaran, 2016). Moreover, the wave periods would be severely underestimated in this case, as the model is not taking care of major swell components from Southern Ocean (Patra and Bhaskaran, 2016). The study by Kumar and Naseef et al. (2015) shows that the annual average H_s is not significantly influenced by the occurrence of one large wave events since the influence such events lasts only 3-4 days. Since the present study deals with only the annual average H_s , the rogue wave events generated below 40° S will not have significant influence on the study results.

5. Conclusion

In the present study, we analyse changes in wave height in the Indian shelf seas using the hindcast data from 1998 to 2012. The annual mean H_s for all the locations in the western shelf seas ($\sim 1.2 \text{ m}$) is slightly higher than that for the locations in the eastern shelf seas ($\sim 1.0 \text{ m}$) due to the stronger influence of summer monsoon in the AS compared to BoB. From 1998 to 2012, the average trend of H_s for all the locations in the western shelf seas is 1.14 cm yr^{-1} and that for the eastern shelf seas is 1.03 cm yr^{-1} . Even though the change in annual average H_s due to tropical cyclone is 2 to 4 cm, it will influence the long-term trend in annual average H_s . The varying bias in the wind speed used for forcing the wave hindcast model also will contribute to the trend estimated. In summary, it is difficult to assess the long-term trend in H_s using a numerical model in a somewhat complex basin, where multiple cyclones are observed annually, primarily, the Bay of Bengal. The short-term sub-synoptic scale wind pulses and fluctuations are not likely to be captured by the numerical model to

the accuracy required for examining the long-term trend. The present study is based on model results obtained by closing the southern boundary at 40° S and can have influence on the wave parameters at different locations in the north Indian Ocean in different seasons and hence the results of this study may be taken into confidence with care.

Acknowledgments

Wave model data was generated under the research project ‘Technical Criteria Atlas (TCA)’ sponsored by the Ministry of Earth Sciences (MoES), Govt. of India. Director, CSIR-National Institute of Oceanography, Goa and Director, National Institute of Ocean Technology, Chennai provided encouragement to carry out the study. We thank all the 3 reviewers for the critical comments which improved the manuscript. This work is NIO contribution number **.

References

- Aarnes, O.J., Abdalla, S., Bidlot, J., Breivik, Ø., 2015. Marine wind and wave height trends at different ERA-Interim forecast ranges. *J. Climate*. 28(2), 819-837.
- Allan, J., Komar, P., 2000. Are ocean wave heights increasing in the eastern North Pacific?. *Eos Trans. AGU*. 81(47), 566–567.
- Amante, C., Eakins, B.W., 2009. ETOPO1 1 arc-minute global relief model: Procedures, data sources and analysis. NOAA Tech. Memo. NESDIS NGDC-24, 19 pp.
- Amrutha, M.M., Kumar, V.S., Anoop, T.R., Nair, T.M.B., Nherakkol, A., Jeyakumar, C., 2014. Waves off Gopalpur, Northern Bay of Bengal during the cyclone PHAILIN. *Annales Geophysicae*. 32(9), 1073-1083. doi:10.5194/angeo-32-1073-2014.
- Anoop, T.R., Kumar, V.S., Shanas, P.R., Glejin, J., 2015. Surface wave climatology and its variability in the North Indian Ocean based on ERA-Interim reanalysis, *J. Atmos. Oceanic Technol.* 32(7), 1372-1385. doi.: 10.1175/JTECH-D-14-00212.1.
- Appendini, C. M., Torres-Freyermuth, A., Salles, P., Lopez- González, J., Mendoza, E.T., 2014. Wave climate and trends for the Gulf of Mexico: A 30-yr wave hindcast. *J. Climate*. 27(4), 1619-1632. doi: 10.1175/JCLI-D-13-00206.1.
- Barstow, S., Mørk, G., Lønseth, L., Mathisen, J.P., 2011. Worldwaves wave energy resource assessments from the deep ocean to the coast. *Journal of Energy and Power Engineering*, 5(8), 730-742.
- Bhaskaran, P.K., Gupta, N., Dash, M.K., 2014. Wind-wave Climate Projections for the Indian Ocean from Satellite Observations. *J. Marine Sci Res Development*. S11,005. doi: 10.4172/2155-9910.S11-005.
- Burkey, J., 2006. A non-parametric monotonic trend test computing Mann-Kendall Tau, Tau-b, and Sen’s Slope written in Mathworks-MATLAB implemented using matrix rotations. King County, Department of Natural Resources and Parks, Science and Technical Services section, Seattle, Washington, USA.

- Carter, D.J.T., Draper, L., 1988. Has the North East Atlantic become rougher?. *Nature*. 332. 494.
- Cavaleri, L., 1994. Wave models and input wind. *Wave Dynamics and Modelling of Ocean Waves*, G. J. Komen et al. Eds., Cambridge University Press, 259–378.
- Clark, C.O., Cole, J.E., Webster, P.J., 2000. Indian Ocean SST and Indian summer rainfall: Predictive relationships and their decadal variability. *J. Climate*. 13(14), 2503–2519.
- DHI., 2011. MIKE 21 SW, User manual, DHI Water and Environment, Denmark.
- Dube, S.K., Sinha, P.C., Rao, A.D., Rao, G.S., 1985. Numerical modelling of storm surges in the Arabian Sea, *Applied Mathematical Modelling* 9. 289-294.
- Findlater, J., 1969. A major low-level air current near the Indian Ocean during the northern summer. *Quart. J. Roy. Meteor. Soc.* 95(404), 362-380. doi:10.1002/qj.49709540409.
- Glejin, J., Kumar, V.S., Nair, T.M.B., Singh, J., 2013. Influence of winds on temporally varying short and long period gravity waves in the near shore regions of the eastern Arabian Sea. *Ocean Sci.* 9(2), 343-353. doi:10.5194/os-9-343-2013.
- Gulev, S.K., Grigorieva, V., 2004. Last century changes in ocean wind wave height from global visual wave data. *Geophysical Research Letters*, 31. L24302. doi: 10.1029/2004GL021040.
- Hemer, M.A., Church, J.A., Hunter, J.R., 2010. Variability and trends in the directional wave climate of the Southern Hemisphere. *Int J. Climatol.* 30(4), 475–491.
- Hinkel, J., Nicholls, R.J., Tol, R.S.J., Wang, Z.B., Hamilton, J.B., Boot, G., Vafeidis, A.T., McFadden, L., Ganopolski, A., and Klein, R. J. T., 2013. A global analysis of erosion of sandy beaches and sea-level rise: An application of DIVA. *Global Planet Change*. 111, 150–158, doi:10.1016/j.gloplacha.2013.09.002.
- Hithin, N.K., Kumar, V.S., Shanab, P.R., 2015. Trends of wave height and period in the Central Arabian Sea from 1996 to 2012: A study based on satellite altimeter data. *Ocean Engg.* 108, 416-425. doi: 10.1016/j.oceaneng.2015.08.024.
- Komen, G.J., Cavaleri, L., Doneland, M., Hasselmann, K., Hasselmann, S., Janssen, P.A.E.M., 1994. *Dynamics and Modelling of Ocean Waves*. Cambridge University Press.
- Kumar, D., Sannasiraj, S.A., Sundar, V., Polnikov, V.G., 2013a. Wind-Wave Characteristics and Climate Variability in the Indian Ocean Region Using Altimeter Data. *Marine Geodesy*. 36(3), 303-318.
- Kumar, V.S., Anoop, T.R., 2015. Spatial and temporal variations of wave height in shelf seas around India. *Natural Hazards*. 78(3), 1693-1706. doi: 10.1007/s11069-015-1796-5.
- Kumar, V.S., Glejin, J., Dora, G.U., Sajiv, C.P., Singh, J., Pednekar, P., 2012. Variations in nearshore waves along Karnataka, west coast of India. *J. Earth System Science*. 121, 393-403.
- Kumar, V.S., Glejin, J., Dubhashi, K.K., Nair, T.M.B., 2013b. Waves during THANE cyclone, Bay of Bengal, *Natural Hazards*. 69, 509-522. doi: 10.1007/s11069-013-0815-7.

- Kumar, V.S., Naseef, T.M., 2015. Performance of ERA-Interim wave data in the nearshore waters around India, *J. Atmos. Oceanic Technol.* 32(6), 1257-1269. doi:10.1175/JTECH-D-14-00153.1.
- Kumar, V.S., Philip, C.S., Nair, T.N.B., 2010. Waves in shallow water off west coast of India during the onset of summer monsoon. *Annales Geophysicae*. 28, 817–824. doi:10.5194/angeo-28-817-2010.
- Nayak, S., Bhaskaran, P.K., Venkatesan, R., Dasgupta, S., 2013. Modulation of local wind waves at Kalpakkam from remote forcing effects of Southern Ocean swells. *Ocean Engg.*, 64, 23-35.
- Patra, A., Bhaskaran, P.K., 2016. Temporal variability in wind-wave climate and its validation with ESSO NIOT wave atlas for the head Bay of Bengal. *Clim. Dyn.*. 1-18. doi 10.1007/s00382-016-3385-z
- Premkumar, K., Ravichandran, M., Kalsi, S.R., Sengupta, D., Gadgil, S., 2000. First results from a new observational system over the Indian Seas. *Curr Sci.*. 78(3), 323-330.
- Trenberth, K.E., 1992. Global analyses from ECMWF and atlas of 1000 to 10 mb circulation statistics. Tech. Rep. NCAR/TN-373+STR, National Center for Atmospheric Research, Boulder, Colorado.
- Semedo, A., Suselj, K., Rutgersson, A., Sterl, A., 2011. A global view on the wind sea and swell climate and variability from ERA-40. *J. Climate*. 24(5), 1461–1479.
- Semedo, A., Weisse, R., Behrens, A., Sterl, A., Bengtsson, L., Gunther, H., 2013. Projection of Global Wave Climate Change toward the End of the Twenty-First Century. *J. Climate*. 26(21), 8269-8288.
- Sen, P.K., 1968. Estimates of the regression coefficient based on Kendall's tau. *J. Amer. Statist. Assoc.*. 63(324), 1379-1389.
- Seneviratne, S.I., et al., 2012. Changes in climate extremes and their impacts on the natural physical environment, in *Managing the Risks of Extreme Events and Disasters to Advance Climate Change Adaptation*, A Special Report of Working Groups I and II of the Intergovernmental Panel on Climate Change., IPCC), edited by C. B. Field et al. pp. 109–230, Cambridge Univ. Press, Cambridge, U. K., and New York.
- Shanas, P.R., Kumar, V.S., 2014. Temporal variations in the wind and wave climate at a location in the eastern Arabian Sea based on ERA-Interim reanalysis data. *Natural Hazards and Earth System Sciences*. 14, 1371–1381, doi:10.5194/nhess-14-1371-2014.
- Shanas, P.R., Kumar, V.S., 2015. Trends in surface wind speed and significant wave height as revealed by ERA-Interim wind wave hindcast in the Central Bay of Bengal. *Int. J. Climatol.* 35, 2654-2663, doi: 10.1002/joc.4164.
- Shankar, D., Shetye, S., 2001. Why is mean sea level along the Indian coast higher in the Bay of Bengal than in the Arabian Sea ?. *Geophysical Research Letters* 28(4), 563–565.
- Sivakholundu, K.M., Jossia, J.K., Jena, B.K., 2014. *Wave Atlas of the Indian Coast*, National Institute of Ocean Technology, Chennai, India, ISBN-81901338-4-5, 130p.
- Sørensen, O.R., Kofoed-Hansen, H., Rugbjerg, M., Sørensen, L.S., 2004. A third-generation spectral wave model using an unstructured finite volume technique. *Proc. 29th Intl. Conf. on Coastal*

Engineering, Lisbon, Portugal, Vol. 29, No. 1, ASCE AMERICAN SOCIETY OF CIVIL ENGINEERS , 894–906.

Stopa, J.E., Cheung, K.F., 2014. Intercomparison of wind and wave data from the ECMWF Reanalysis Interim and the NCEP Climate Forecast System Reanalysis. *Ocean Modell.*, 75, 65-83. doi: 10.1016/j.ocemod.2013.12.006.

Sundar, V., 1986. Wave characteristics off the South East Coast of India. *Ocean Engg.*. 13(4), 327-338.

Young, I.R., 1999. Seasonal variability of the global ocean wind and wave climate. *Int. J. Climatol.*. 19, 931–950.

Young, I.R., Zieger, S., Babanin, A., 2011. Global trends in wind speed and wave height. *Science*. 332(6028)., 451–455.

Figure captions

Figure 1. Map showing the model domain and the 19 locations studied in the shelf seas around Indian mainland. AD02 and DS3 are buoy measurement locations used in the study. DS1 buoy location is 0.5 deg east of AD02

Figure 2. Plot of hindcast significant wave height (H_s) with measured values at a) AD02 (Arabian Sea) and b) DS3 (Bay of Bengal) locations for 6 hr interval data. c) and d) are for monthly mean data at AD02 and DS3. The dashed line indicate the 15% deviation from the exact match line. Exact match line is shown as solid line. a and c are for the year 2012 and b and d are for 2003

Figure 3. Comparison of hindcast significant wave height at AD02 (Arabian Sea) during February-December 2012 based on domain restriction at 40° S and without domain restriction in the south.

Figure 4. Plot of monthly mean H_s at different locations from 1998 to 2012.

Figure 5. Seasonal average mean significant wave height based on data from 1998 to 2012. a) non-monsoon, b) summer monsoon and c) winter monsoon. All the values are in meter

Figure 6. Plot of monthly maximum H_s at different locations from 1998 to 2012.

Figure 7. Trend of annual mean H_s during 1998 to 2012 at locations 1 to 19. The solid line is the data and the dotted line is the linear fit.

Figure 8. Comparison of H_s estimated based on numerical model and that from ERA-I. The solid line indicates the exact match and the dotted line is 15% deviation.

Figure 9. Scatter plot of measured and the hindcast values during tropical cyclone Thane. Top panel shows the comparison of significant wave height and the bottom panel is mean wave period.

Table 1. Results of the sensitivity analysis carried out by varying the southern model boundary

Parameter	Location	Statistics	30° S	40° S	50° S	60° S	70° S
Significant Wave Height	Arabian Sea	Correlation Coefficient	0.975	0.977	0.970	0.968	0.970
		MAE (m)	0.417	0.341	0.316	0.312	0.308
		RMSE (m)	0.545	0.485	0.463	0.447	0.451
	Bay of Bengal	Correlation Coefficient	0.916	0.899	0.882	0.882	0.887
		MAE (m)	0.538	0.443	0.356	0.32	0.327
		RMSE (m)	0.671	0.574	0.493	0.448	0.463
Mean Wave Period	Arabian Sea	Correlation Coefficient	0.838	0.901	0.888	0.884	0.895
		MAE (s)	0.746	0.544	0.524	0.569	0.518
		RMSE (s)	1.013	0.721	0.713	0.785	0.719
	Bay of Bengal	Correlation Coefficient	0.590	0.627	0.61	0.567	0.631
		MAE (s)	1.357	0.940	0.932	1.082	0.971
		RMSE (s)	1.403	1.019	1.319	1.23	0.988

MAE - mean absolute error

RMSE - root mean square error

Table 2. Average Hs during different months at the locations studied

Location No.	Location		Monthly average Hs (m)											
	Longitude (Deg E)	Latitude (Deg N)	Month											
			Jan	Feb	Mar	Apr	May	Jun	Jul	Aug	Sep	Oct	Nov	Dec
1	68.25	22.50	0.67	0.72	0.82	0.99	1.34	2.00	2.37	1.97	1.29	0.85	0.70	0.68
2	69.00	21.00	0.77	0.80	0.87	0.99	1.31	2.18	2.71	2.25	1.42	0.90	0.79	0.77
3	71.25	19.50	0.73	0.73	0.80	0.89	1.18	2.11	2.60	2.18	1.41	0.82	0.72	0.70
4	72.00	18.00	0.75	0.77	0.81	0.84	1.10	2.10	2.56	2.12	1.39	0.83	0.72	0.71
5	72.75	16.50	0.72	0.77	0.80	0.83	1.07	2.05	2.46	2.00	1.34	0.82	0.69	0.67
6	73.50	15.00	0.69	0.75	0.78	0.80	1.06	2.00	2.36	1.89	1.30	0.81	0.67	0.65
7	73.50	13.50	0.76	0.82	0.86	0.90	1.15	2.14	2.46	1.97	1.42	0.95	0.81	0.76
8	74.25	12.00	0.70	0.78	0.85	0.90	1.18	2.09	2.33	1.88	1.42	0.99	0.79	0.70
9	75.00	10.50	0.72	0.78	0.86	0.93	1.23	2.02	2.20	1.81	1.44	1.05	0.83	0.77
10	75.75	9.00	0.68	0.76	0.87	0.96	1.29	1.96	2.10	1.76	1.46	1.12	0.84	0.72
11	77.25	7.50	1.27	1.12	0.99	1.05	1.49	2.02	2.13	1.86	1.61	1.28	1.10	1.28
12	81.00	10.50	1.06	0.92	0.77	0.79	1.16	1.26	1.16	1.15	1.08	0.91	1.03	1.23
13	81.00	12.00	0.97	0.86	0.77	0.82	1.13	1.19	1.11	1.10	1.00	0.88	1.05	1.19
14	81.00	13.50	0.87	0.80	0.78	0.88	1.06	1.07	1.03	1.01	0.93	0.86	1.03	1.09
15	81.00	15.00	0.78	0.76	0.79	0.91	1.04	1.07	1.07	1.04	0.93	0.86	0.97	0.96
16	83.00	16.50	0.76	0.74	0.79	0.95	1.21	1.40	1.42	1.38	1.17	0.99	0.98	0.94
17	85.00	18.50	0.63	0.68	0.86	1.12	1.31	1.49	1.50	1.42	1.20	0.93	0.78	0.71
18	87.00	19.50	0.55	0.57	0.80	1.13	1.35	1.66	1.67	1.55	1.25	0.89	0.68	0.62
19	88.50	20.25	0.50	0.50	0.74	1.10	1.33	1.72	1.74	1.60	1.28	0.87	0.61	0.55

Table 3. Mean and maximum H_s during summer monsoon, winter monsoon, non-monsoon and annual mean H_s at the locations studied

Location	non-monsoon		summer monsoon		winter monsoon		annual	
	mean (m)	maximum (m)	mean (m)	maximum (m)	mean (m)	maximum (m)	mean (m)	maximum (m)
1	1.0	2.8	1.9	5.9	0.7	2.4	1.2	5.9
2	1.0	3.0	2.1	7.4	0.8	2.6	1.3	7.4
3	0.9	3.3	2.1	5.7	0.7	3.2	1.2	5.7
4	0.9	3.1	2.0	6.5	0.8	3.6	1.2	6.5
5	0.9	3.5	2.0	6.2	0.7	3.5	1.2	6.2
6	0.9	4.7	1.9	5.9	0.7	4.0	1.1	5.9
7	0.9	4.5	2.0	5.7	0.8	3.2	1.3	5.7
8	0.9	4.0	1.9	5.0	0.8	2.9	1.2	5.0
9	1.0	4.5	1.9	4.7	0.8	2.4	1.2	4.7
10	1.0	4.1	1.8	4.2	0.8	2.4	1.2	4.2
11	1.2	3.4	1.9	3.7	1.2	2.8	1.4	3.7
12	0.9	2.5	1.2	2.6	1.0	4.3	1.0	4.3
13	0.9	3.3	1.1	2.3	1.0	5.9	1.0	5.9
14	0.9	5.4	1.0	2.5	0.9	5.1	1.0	5.4
15	0.9	5.1	1.0	2.9	0.9	4.3	0.9	5.1
16	0.9	4.4	1.3	4.4	0.9	3.6	1.1	4.4
17	1.0	3.1	1.4	5.0	0.7	2.9	1.1	5.0
18	1.0	3.6	1.5	5.2	0.7	3.8	1.1	5.2
19	0.9	5.9	1.6	6.0	0.6	4.7	1.0	6.0

Table 4. Trend of monthly average H_s (cm/yr) at the locations studied

Location	Jan	Feb	Mar	Apr	May	June	Jul	Aug	Sep	Oct	Nov	Dec
1	0.50	0.00	1.10	-0.10	1.33	3.25	2.00	1.88	2.00	0.33	1.38	1.50
2	1.07	-0.11	1.00	0.50	0.50	3.00	3.17	2.60	3.17	0.90	1.55	1.43
3	1.60	0.60	0.80	0.91	-0.58	2.14	2.33	3.00	3.50	0.67	1.30	0.63
4	1.33	0.40	0.56	1.11	-1.00	2.00	2.29	2.38	3.54	0.57	1.21	0.56
5	1.00	0.50	0.67	0.89	-0.60	1.62	2.29	2.50	4.00	0.67	1.36	0.75
6	1.17	0.78	0.50	1.00	-0.50	1.20	2.00	2.38	3.67	0.71	1.62	1.00
7	1.42	0.50	0.50	1.00	-0.75	1.11	1.60	1.45	3.83	0.86	2.38	1.43
8	1.36	0.38	0.71	1.00	-0.82	0.25	0.80	0.27	3.08	0.80	2.00	1.33
9	1.82	0.62	1.00	1.00	-0.88	0.00	0.50	-0.11	3.00	0.50	2.20	1.43
10	0.16	0.58	0.91	1.40	-0.91	-0.25	0.27	-0.30	2.80	0.20	2.00	1.58
11	0.31	2.71	1.60	1.60	0.00	0.00	1.00	0.00	2.78	-0.17	2.64	2.90
12	0.64	0.38	0.00	0.50	2.40	1.50	1.57	1.23	1.56	1.50	1.33	1.50
13	0.33	0.50	0.17	0.60	2.50	0.50	0.75	0.63	1.08	1.10	1.44	1.17
14	0.33	-0.13	0.00	0.60	2.08	0.50	1.00	1.00	1.15	0.67	1.50	1.50
15	0.80	-0.14	-0.29	0.50	2.00	0.75	0.89	0.86	1.13	0.50	1.50	1.75
16	1.00	0.00	0.40	0.60	1.80	1.44	2.00	1.20	1.85	0.71	1.60	1.33
17	0.83	0.44	1.00	0.67	1.50	2.00	3.33	2.00	2.75	0.33	1.50	0.75
18	0.20	0.00	1.29	0.00	0.83	1.25	3.17	2.20	2.83	0.00	0.50	0.00
19	-0.17	-0.10	1.40	0.29	0.80	1.60	2.93	2.25	3.43	0.00	0.00	-0.25

Table 5. Trend of mean H_s during the summer monsoon, winter monsoon, non-monsoon and annual period along with the trend of annual mean wind speed

Location	non-monsoon mean H_s (cm/yr)	summer monsoon mean H_s (cm/yr)	winter monsoon mean H_s (cm/yr)	annual mean H_s (cm/yr)	annual mean wind speed (cm/s/yr)
1	0.44	2.21	0.85	1.18	2.20
2	0.37	2.79	1.14	1.43	0.56
3	0.39	2.36	0.86	1.21	2.69
4	0.31	2.49	0.77	1.21	0.31
5	0.26	2.49	0.80	1.20	2.79
6	0.42	2.28	0.94	1.21	2.51
7	0.40	1.68	1.20	1.10	0.02
8	0.43	1.08	1.17	0.88	1.10
9	0.53	0.70	1.24	0.85	-0.21
10	0.55	0.66	1.22	0.82	-0.05
11	1.34	0.83	2.14	1.47	6.49
12	0.93	1.39	1.17	1.19	3.02
13	0.81	0.76	1.10	0.92	-0.19
14	0.67	0.84	1.17	0.88	-0.63
15	0.53	0.86	1.14	0.86	-1.36
16	0.65	1.44	1.14	1.06	0.69
17	1.03	2.45	0.89	1.46	4.92
18	0.56	2.28	0.22	0.99	0.45
19	0.59	2.15	-0.02	0.90	0.57

Table 6. Annual average wind speed from buoy and ECMWF

Sl No.	Buoy-Id (position)	Year	Annual average - buoy (m/s)	Annual average- ECMWF (m/s)	Percentage difference	Collocated Points
1.	DS1 (15.5N, 69.2E)	1998	5.66	5.58	-1.4	1044
2.	AD02 (15.0N, 69.0E)	2011	5.43	6.28	15.7	1423
3.	AD02 (15.0N, 69.0E)	2012	5.65	6.33	12.0	1456

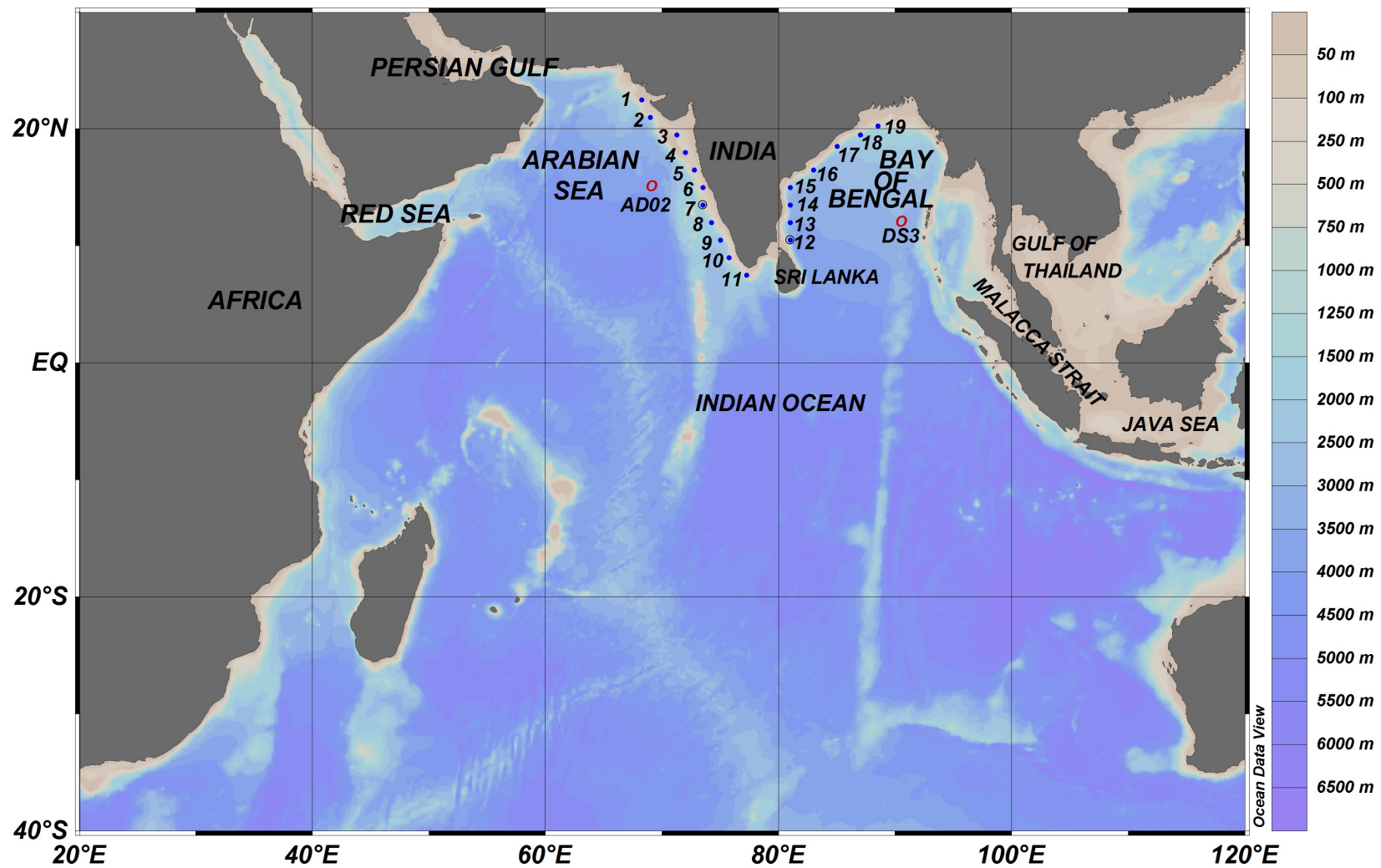


Figure 1. Map showing the model domain and the 19 locations studied in the shelf seas around Indian mainland. AD02 and DS3 are buoy measurement locations used in the study. DS1 buoy location is 0.5 deg east of AD02

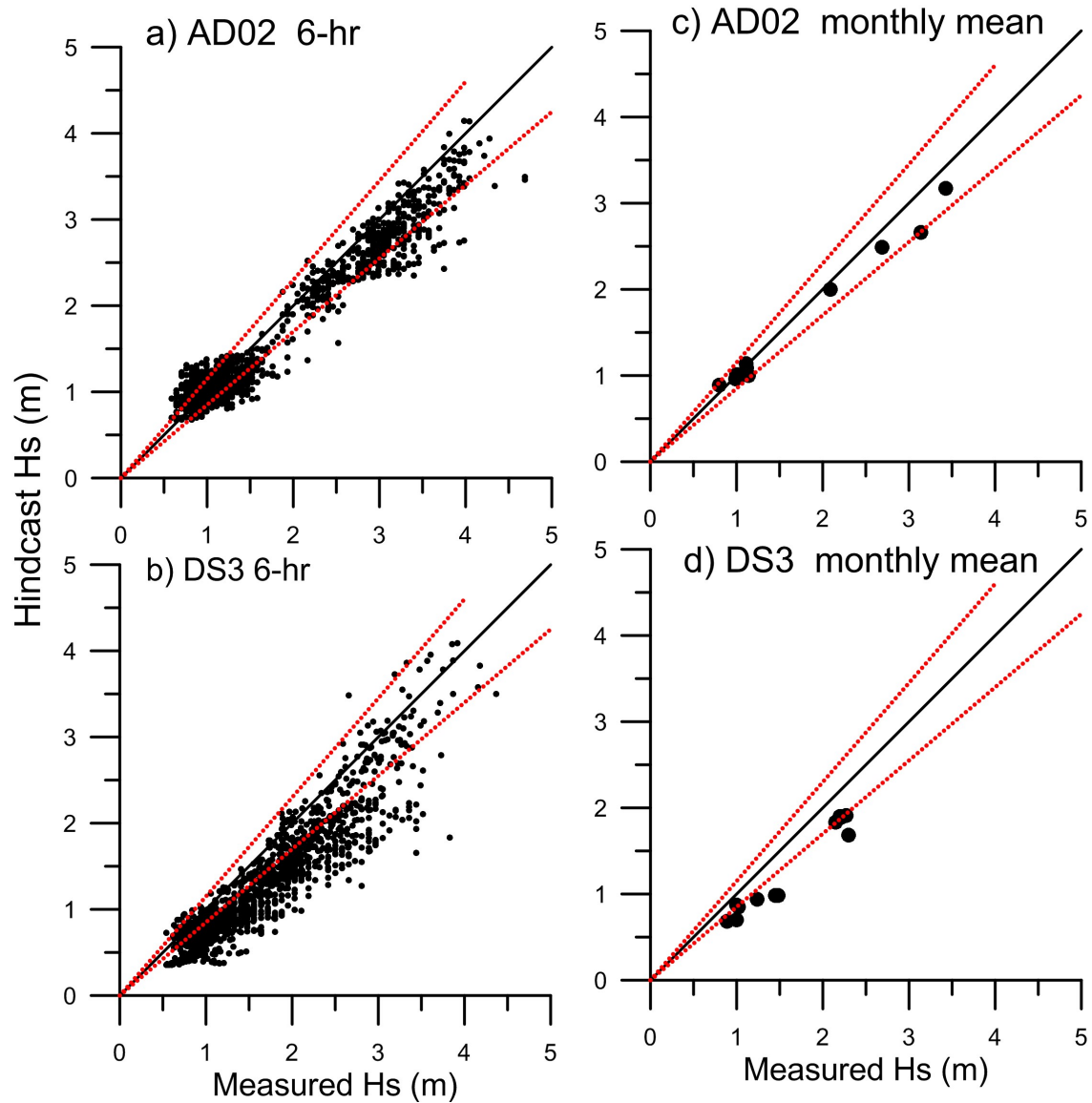


Figure 2. Plot of hindcast significant wave height (H_s) with measured values at a) AD02 (Arabian Sea) and b) DS3 (Bay of Bengal) locations for 6 hr interval data. c) and d) are for monthly mean data at AD02 and DS3. The dashed line indicate the 15% deviation from the exact match line. Exact match line is shown as solid line. a and c are for the year 2012 and b and d are for 2003

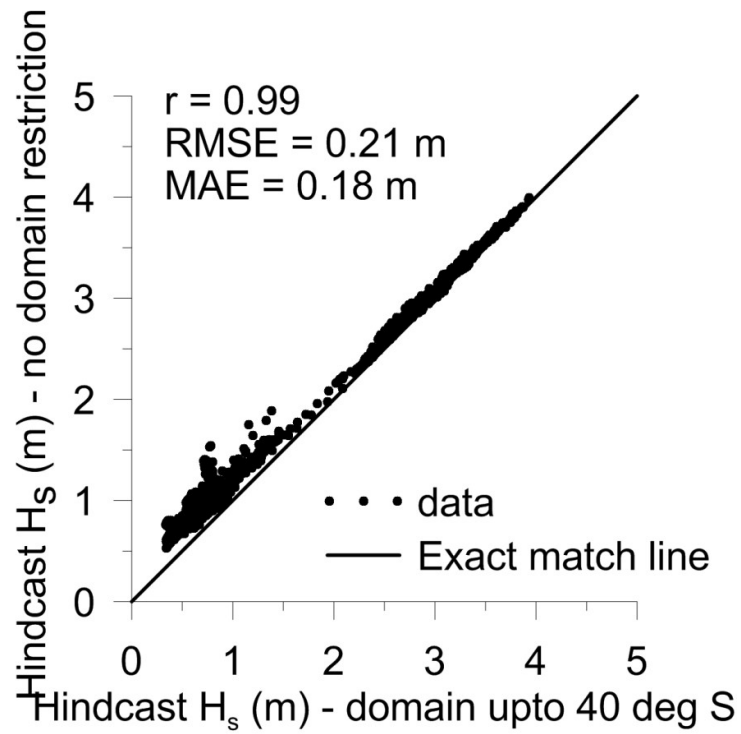


Figure 3. Comparison of hindcast significant wave height at AD02 (Arabian Sea) during February-December 2012 based on domain restriction at 40° S and without domain restriction in the south

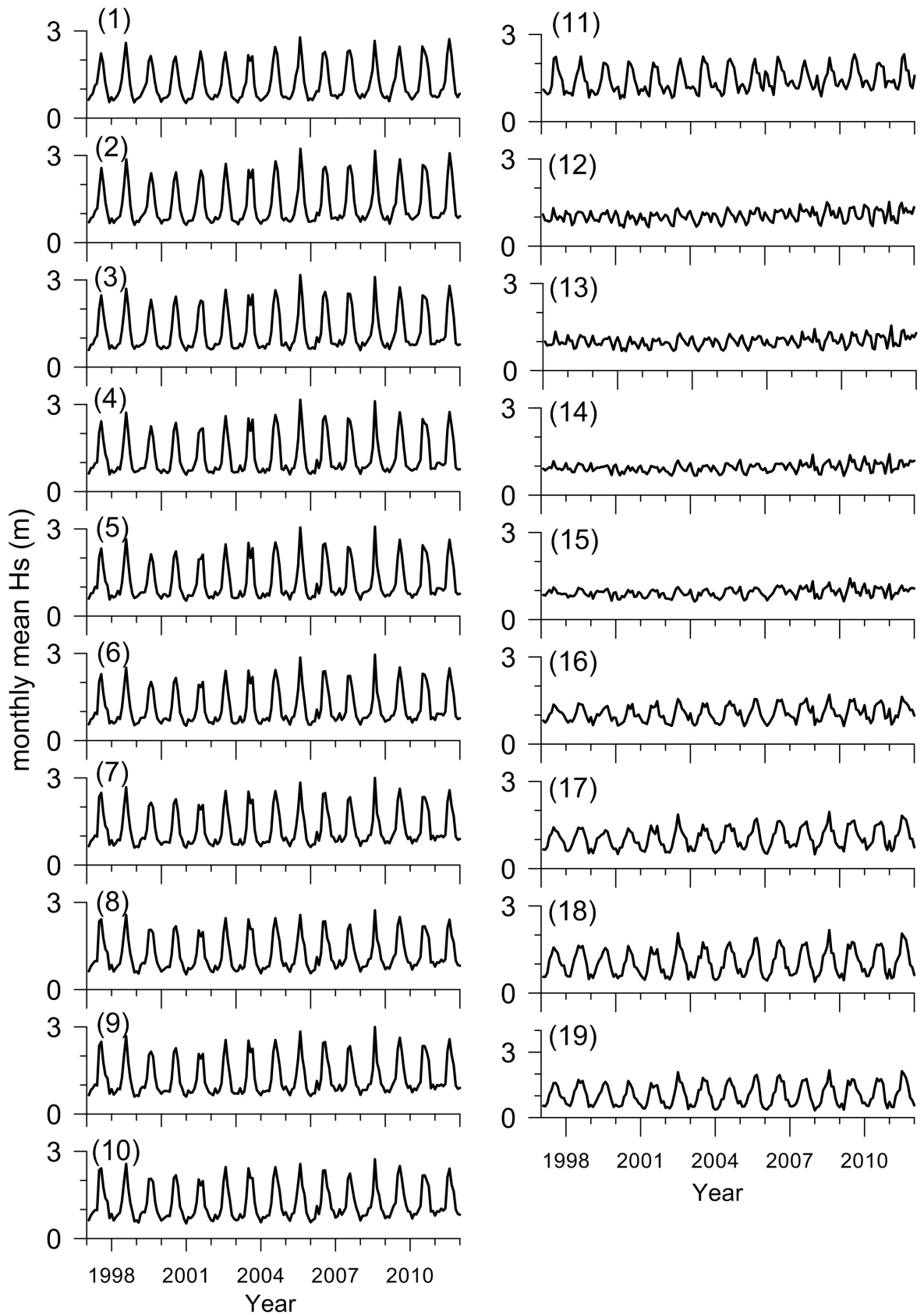


Figure 4. Plot of monthly mean H_s at different locations from 1998 to 2012

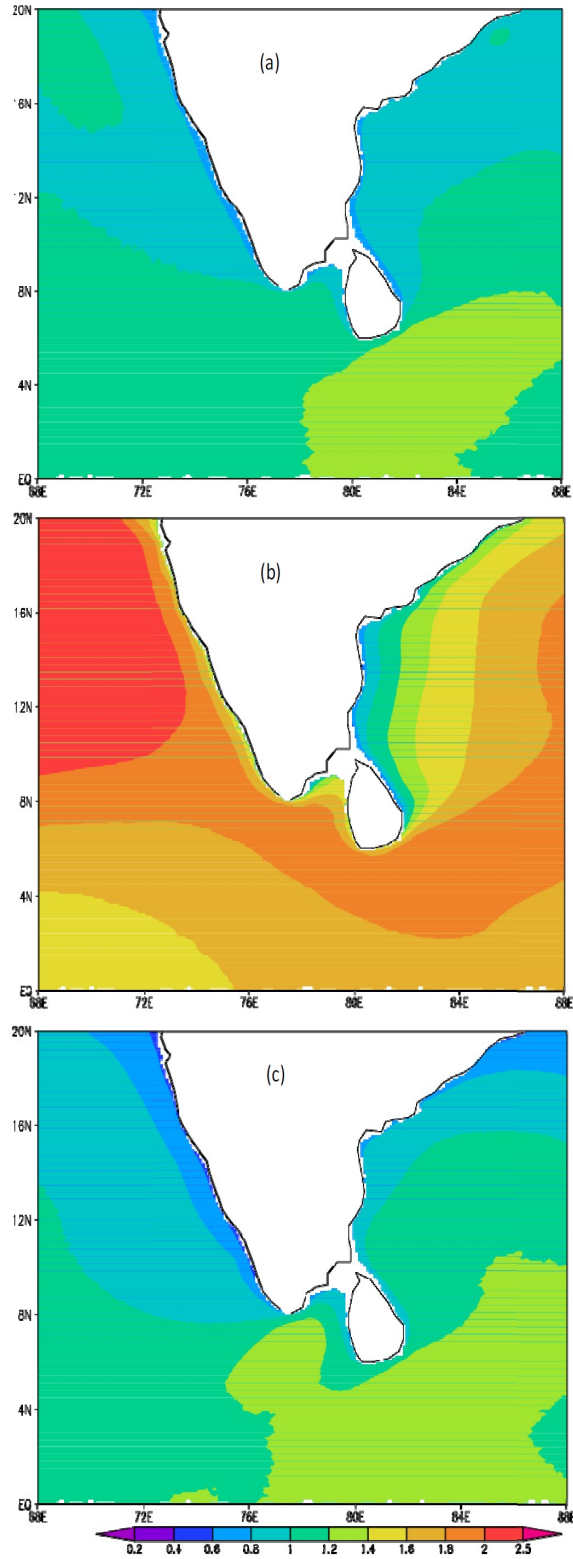


Figure 5. Seasonal average mean significant wave height based on data from 1998 to 2012. a) non-monsoon, b) summer monsoon and c) winter monsoon. All the values are in meter

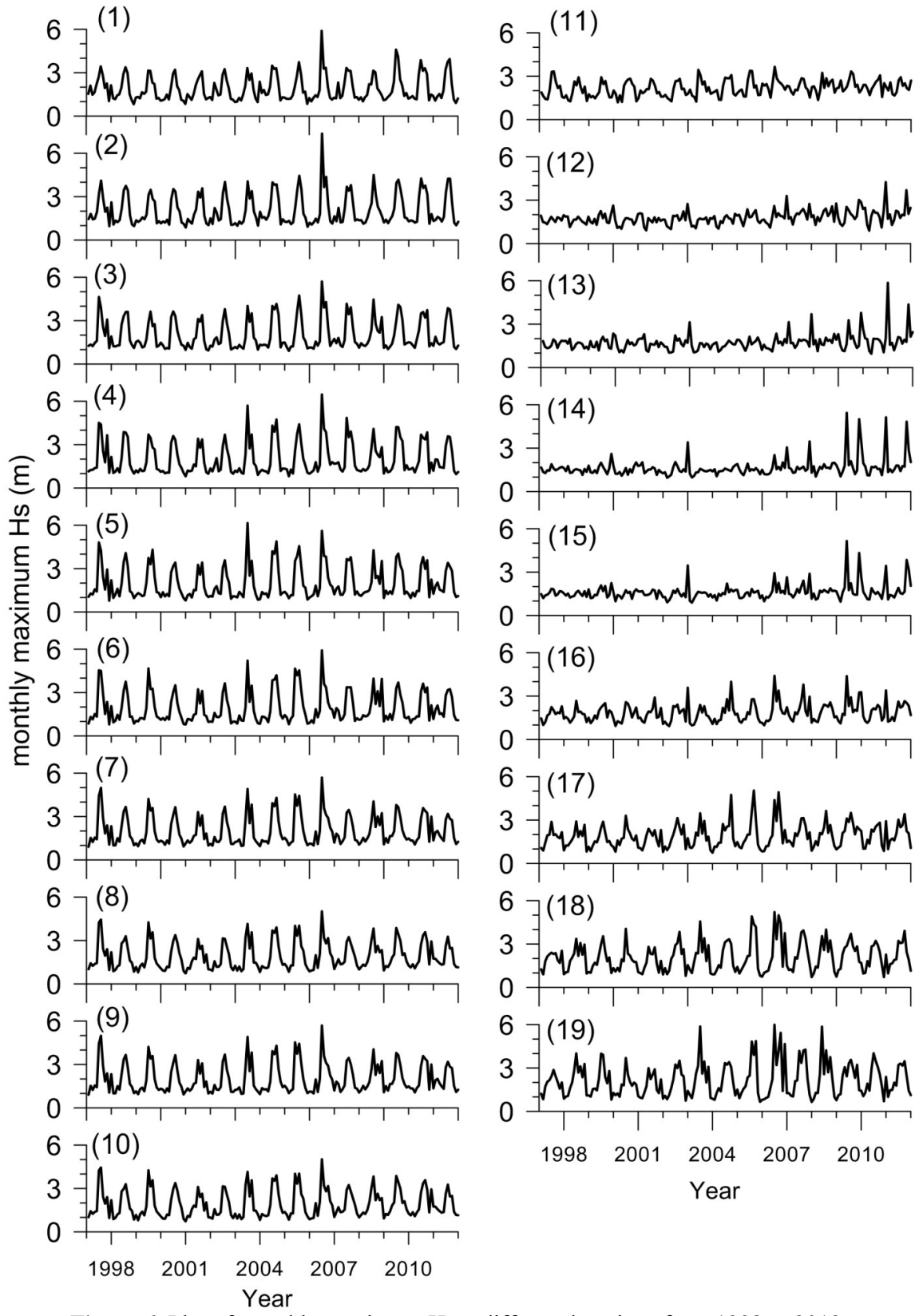


Figure 6. Plot of monthly maximum H_s at different locations from 1998 to 2012

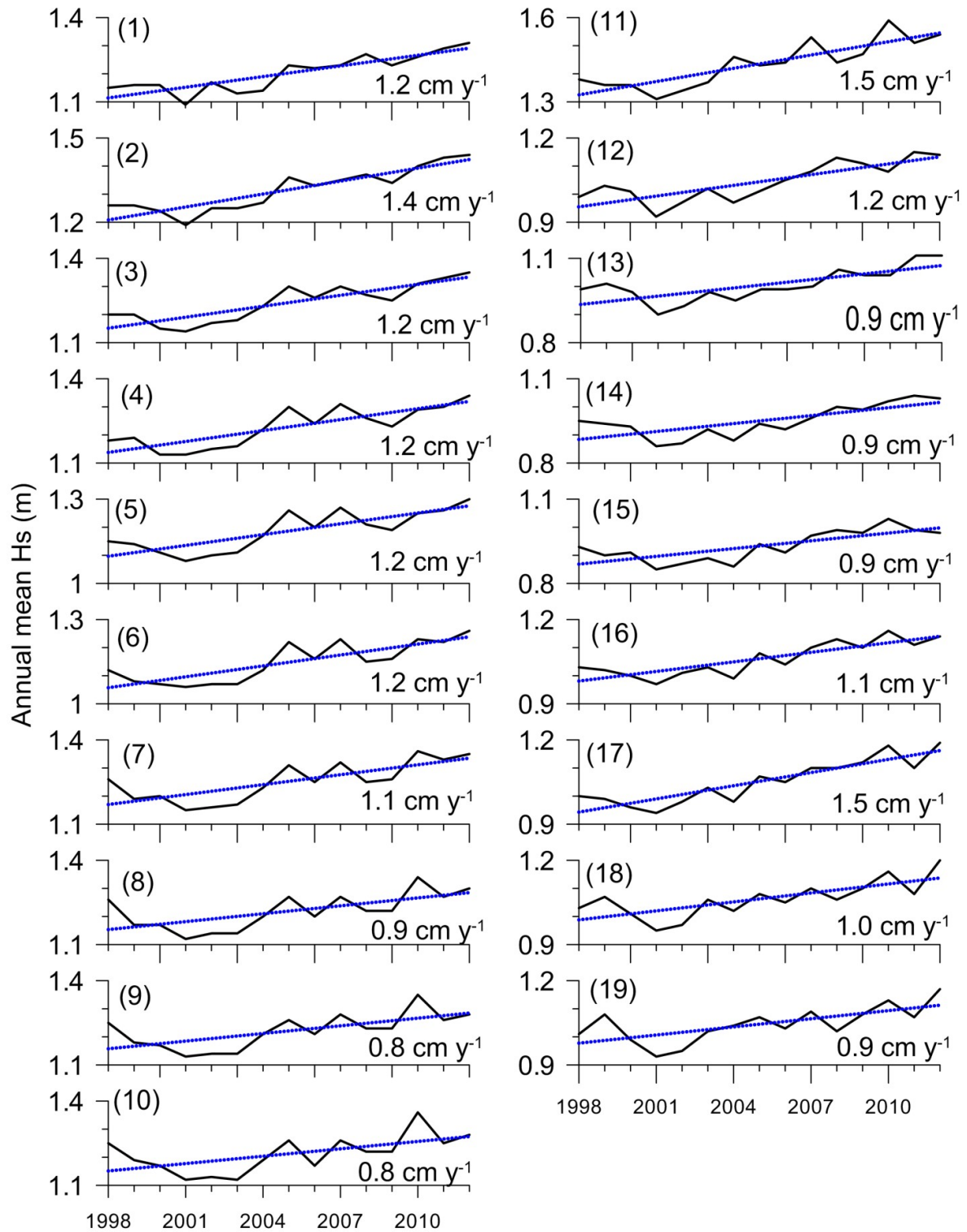


Figure 7. Trend of annual mean H_s during 1998 to 2012 at locations 1 to 19. The solid line is the data and the dotted line is the linear fit

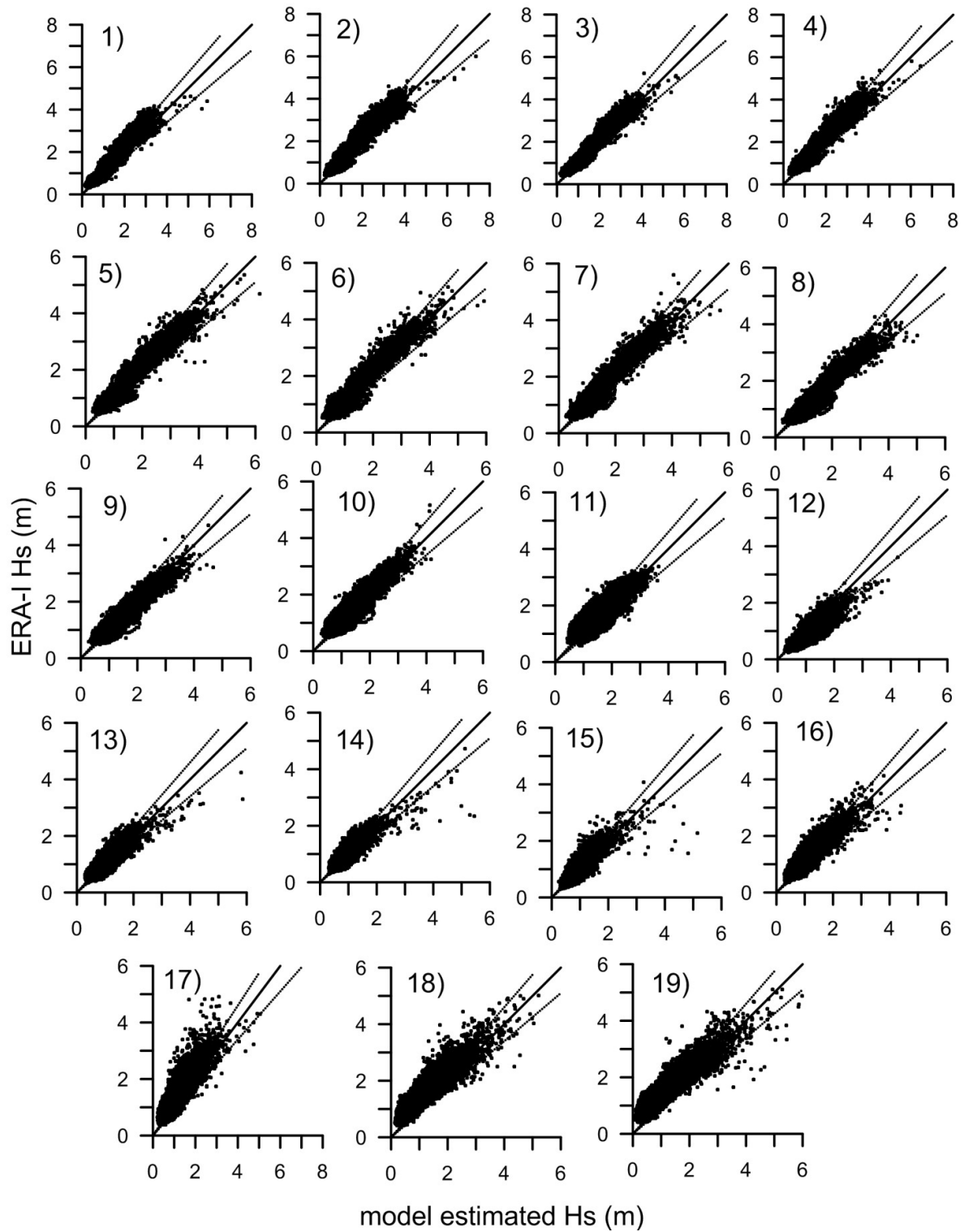


Figure 8. Comparison of H_s estimated based on numerical model and that from ERA-I. The solid line indicates the exact match and the dotted line is 15% deviation

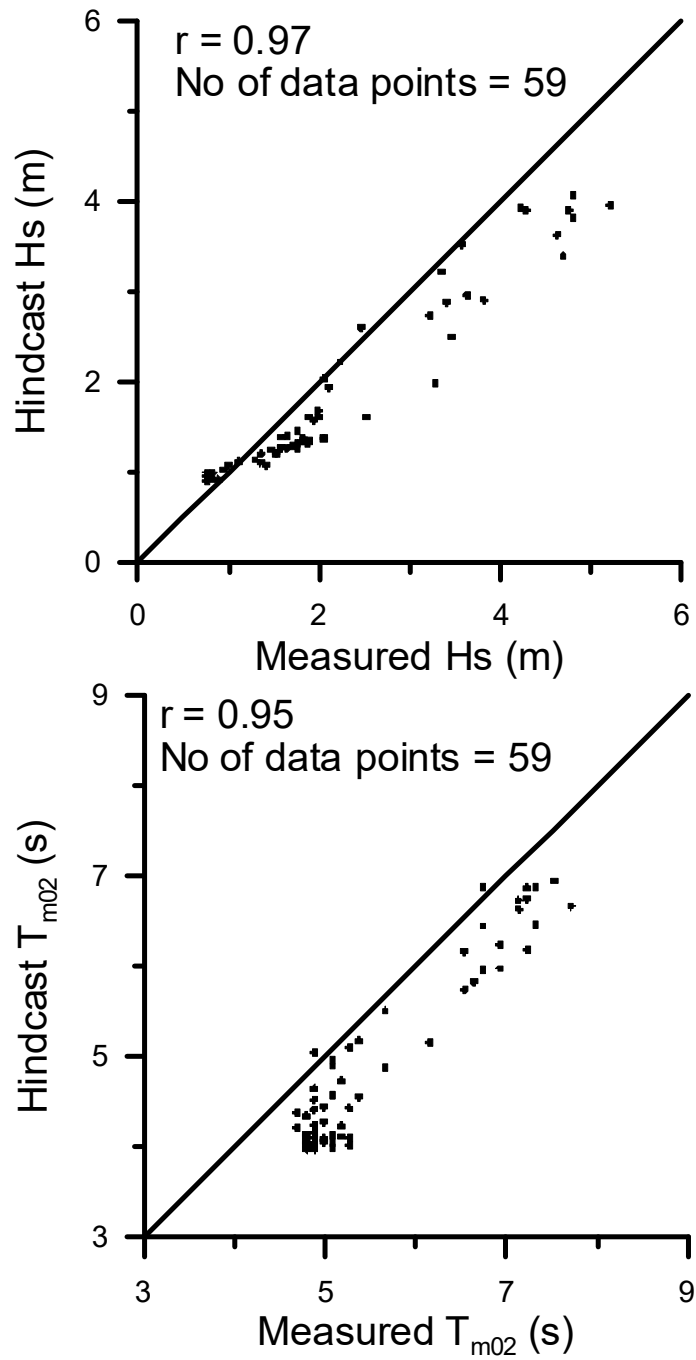


Figure 9. Scatter plot of measured and the hindcast values during tropical cyclone Thane. Top panel shows the comparison of significant wave height and the bottom panel is mean wave period